Vol. 523: 93–103, 2015
doi: 10.3354/meps11199

MARINE ECOLOGY PROGRESS SERIES
Mar Ecol Prog Ser

Published March 16

Changes in pteropod distributions and shell dissolution across a frontal system in the California Current System

N. Bednaršek[1,3,*], M. D. Ohman[2]

[1]Pacific Marine Environmental Laboratory (PMEL), National Oceanic and Atmospheric Administration (NOAA), 7600 Sand Point Way NE, Seattle, WA 98115, USA

[2]California Current Ecosystem LTER site, Scripps Institution of Oceanography, University of California San Diego, 9500 Gilman Drive, La Jolla, CA 92093-0218, USA

[3]*Present address:* School of Marine and Environmental Affairs, University of Washington, 3707 Brooklyn Ave NE, Seattle, WA 98105, USA

ABSTRACT: We tested the sensitivity of the vertical distributions and shell dissolution patterns of thecosome pteropods to spatial gradients associated with an eddy-associated front in the southern California Current System. The aragonite saturation horizon (Ω_{arag} = 1.0) shoaled from >200 to <75 m depth across the front. The vertical distribution of thecosome pteropods tracked these changes, with all 5 species showing reduced occurrence at depths below 100 m where waters were less saturated with respect to aragonite. Shell dissolution patterns of the numerically dominant thecosome *Limacina helicina* corresponded to the cross-frontal changes in Ω_{arag} saturation state. Severe shell dissolution (categorized here as Type II and Type III) was low in near-surface waters where Ω_{arag} > 1.4, while peak dissolution occurred in depths where Ω_{arag} = 1.0 to 1.4. Vertical habitat compression and increased shell dissolution may be expected to accompany future shoaling of waters that are undersaturated with respect to aragonite.

KEY WORDS: Pteropoda · Ocean fronts · Vertical distribution · Shell dissolution

INTRODUCTION

Carbon dioxide (CO_2) uptake from the atmosphere leads to a process commonly referred to as ocean acidification, resulting in a reduction of seawater pH and in saturation state with respect to aragonite and calcite, the 2 most common polymorphs of calcium carbonate ($CaCO_3$) formed by marine organisms (Feely et al. 2004, Orr et al. 2005, Fabry et al. 2008, Doney et al. 2009). A decline in saturation state results in a greater frequency of thermodynamically unfavorable conditions for precipitation of $CaCO_3$ and the potential for enhanced dissolution of $CaCO_3$ in the water column (Fassbender et al. 2011, Harris et al. 2013, Lachkar 2014). The term that quantifies the thermodynamic tendency toward dissolution or precipitation is the saturation state (Ω) for a given $CaCO_3$ mineral (e.g. aragonite): $\Omega_{arag} = [Ca^{2+}][CO_3^{2-}]/K'_{sp,arag}$, where $[Ca^{2+}]$ and $[CO_3^{2-}]$ are concentrations of calcium and carbonate ions, respectively, and $K'_{sp,arag}$ is the apparent solubility product for aragonite. When Ω_{arag} is greater (less) than 1, precipitation (dissolution) is thermodynamically favored.

Among the sources of climate forcing affecting the coastal upwelling ecosystem of the California Current System (Chan et al. 2008, Di Lorenzo & Ohman 2013, Bograd et al. 2014), the consequences of changes in the carbonate system chemistry are some of the least well understood. Early models projected that waters undersaturated with respect to aragonite

*Corresponding author: nina.bednarsek@noaa.gov

might reach the sea surface in parts of the North Pacific by the year 2100 (Orr et al. 2005). However, *in situ* measurements have revealed that during the upwelling season, undersaturated waters already occur near or even at the sea surface (Feely et al. 2008, Alin et al. 2012, Harris et al. 2013, Ohman et al. 2013b, Martz et al. 2014). While coastal upwelling naturally brings high pCO_2, low pH, undersaturated waters close to the sea surface (Alin et al. 2012) and has done so since the pre-industrial era, anthropogenic increases in CO_2 in upwelled source waters are now exacerbating the magnitude of undersaturation and expanding the vertical extent of potentially corrosive waters (Feely et al. 2008, Harris et al. 2013).

Observations and updated modeling predictions show a progressive temporal decline in saturation state in the California Current Ecosystem (Hauri et al. 2009, 2013, Rykaczewski & Dunne 2010, Gruber et al. 2012, Lachkar 2014). Lachkar (2014) suggested that while 10% of southern California habitat in the upper 200 m is currently undersaturated with respect to aragonite, a doubling of atmospheric CO_2 could lead to an increase to approximately 75% of this habitat being undersaturated during the summer upwelling season. The consequences for shell-secreting marine organisms in this region are only beginning to be understood, but include deleterious effects on survivorship of oyster larvae at commercial hatcheries (e.g. Barton et al. 2012, Waldbusser et al. 2013).

Shelled pteropods (thecosomes) and heteropods are free-swimming pelagic molluscs that make thin shells out of aragonite. Their shells are thought to undergo rapid shell dissolution at $\Omega_{arag} < 1$, making them among the first taxa to be vulnerable to the progressive increase in corrosive waters (Feely et al. 2004, Orr et al. 2005, Bednaršek et al. 2012a, 2014). Their responses include increased larval dissolution and reduced calcification (Comeau et al. 2009, 2010, Lischka et al. 2011), reduced weight and incremental shell length (Comeau et al. 2009, Roberts et al. 2011), and diminished mechanical properties (Teniswood et al. 2013). Pteropods and heteropods are part of the mesozooplankton community in the southern California Current Ecosystem (Lavaniegos & Ohman 2007, Ohman et al. 2009). Studies have shown the importance of pteropods to vertical carbon export via their high sinking rates (Accornero et al. 2003, Manno et al. 2010), ballasting effects, mucus feeding webs, and vertical migration below the mixed layer (Lalli & Gilmer 1989). Yet, whether thecosome pteropods in the California Current System have already been affected by the effects of changing carbonate chemistry has not been demonstrated unequivocally. Bednaršek et al. (2014) linked lowered Ω_{arag} along nearshore regions of the California Current System to evidence of extensive pteropod shell dissolution in the corrosive waters of the natural environment. That study also suggested a causal relationship between shell dissolution and increased mortality. Ohman et al. (2009) could not detect declines in abundance of pteropods or heteropods in either southern or central California waters, based on a 58 yr record of observations from the CalCOFI program. However, they were not able to assess changes in vertical distributions, shell morphology, or structural properties, and projected that changes in abundance would become detectable with time. Mackas & Galbraith (2012) reported an increase in 2 species of pteropods (1 thecosome, 1 gymnosome) and a decline in 1 thecosome species off Vancouver Island. The authors concluded that such changes were not attributable to ocean acidification.

Pteropods have not been successfully cultivated in experimental conditions beyond 3 or 4 wk (Lischka et al. 2011). Even mesocosm experiments are not successful at reproducing natural pteropod responses (Niehoff et al. 2013, Schulz 2013). Exploiting natural gradients in the ocean provides an alternative approach for understanding the susceptibility of pteropods to changes in ocean carbon geochemistry. Toward this end, we investigated the response of thecosome pteropods to a relatively abrupt spatial gradient in aragonite saturation horizons associated with a frontal system in the California Current System. We tested the hypothesis that the composition of the pteropod assemblage, the vertical distribution of the animals, and their shell dissolution patterns would respond to a marked spatial change in aragonite saturation horizons across the frontal system.

MATERIALS AND METHODS

Front identification and sampling

A frontal gradient designated the 'E-Front' (eddy front) was located approximately 200 km west of Pt. Conception in the southern California Current System (see Fig. 1a,c). It was initially identified using AVISO (Archiving, Validation, and Interpretation of Satellite Oceanographic data) sea surface height satellite imagery, followed by *in situ* profiling using a SeaSoar (Johnston et al. 2011) and Moving Vessel Profiler (Ohman et al. 2013b). An initial SeaSoar survey was completed between 30 July and 2 August

2012, tow-yowing between 300 m and just below the sea surface (Ohman et al. 2013a). SeaSoar instrumentation included calibrated dual Seabird conductivity (SBE4C) and temperature (SBE3Plus) sensors, a Seabird SBE9Plus pressure sensor, a calibrated Rinko3 dissolved oxygen optode sensor (JFE Advantech), and a Laser Optical Particle Counter (data not shown). Dissolved oxygen and temperature data were then used to calculate Ω_{arag} from the proxy relationship developed for this ocean region by Alin et al. (2012, their Table 1, Eq. 2). However, Ω_{arag} estimated by proxy relationships has a higher uncertainty in the upper 15 to 20 m of the water column (Alin et al. 2012). Vertically stratified samples of pteropods were taken using a 202 µm mesh, 1 m^2 MOCNESS (Wiebe et al. 1985), at 4 locations. Two MOCNESS tows (6 and 8) were taken east of the E-Front in a region (designated Cycle 3), while 2 tows (10 and 12) were taken west of the E-Front at Cycle 4 (see Fig. 1c). Cycles refer to repeated cycles of activity associated with Lagrangian drifter stations while following a water parcel. MOCNESS sampling was done during daylight hours (12:20 to 14:00 h local time), in 100 m strata from 400 to 300 m, 50 m strata from 300 to 100 m, and 25 m strata from 100 to 0 m. Daytime was selected in order to capture the maximum depth distribution of the pteropods over a diel cycle. The MOCNESS included a SBE3 temperature, SBE4 conductivity, SBE43 dissolved oxygen, and Wetlabs CST-479DR beam transmissometer, all calibrated. Upon recovery, MOCNESS samples were promptly preserved in 95% non-denatured ethanol with 5 mM NH_4OH added to maintain pH at ~8.5 to protect pteropod shells from dissolution. The ethanol solution was drained and replaced within 24 h of initial preservation.

Pteropod and shell dissolution analysis

Pteropods and atlantid heteropods were enumerated from entire MOCNESS samples using a dissecting microscope and identified to the species level. Gymnosome pteropods and carinariid or pterotrachiid heteropods were rare and thus were not enumerated. The pteropod *Limacina helicina* (Phipps, 1774) was the most numerous thecosome found, and was analyzed in detail for evidence of shell dissolution using scanning electron microscopy (SEM). Dissolution was analyzed from an average of 10 individuals (range 2 to 15, based on availability of specimens) of *L. helicina* at each depth at both cycles (tows 6 and 10), totaling 166 individuals. We used a non-destructive preparation method on preserved specimens prior to examining shell surfaces (Bednaršek et al. 2012c). A 2-step preparation method of dehydration and drying is necessary in order to avoid artefacts of shell damage created by shear vacuum forces inside the SEM. First, 6% H_2O_2 was used to remove any abiogenic crystal precipitates on the shell. This step was followed by dehydration using 2,2 dimetoxypropane and 1,1,1,3,3,3-hexamethyldisilazane. Previous work demonstrated that these chemical treatments do not introduce additional shell dissolution (Bednaršek et al. 2012c). Second, plasma etching was applied to remove upper organic layers and expose the structural elements of the shell. PT7150 and PT7300 plasma etchers were used with a forward power of ~200 W and a reflected power of ~5 W, usually for between 10 and 30 min, depending on the efficiency of the etcher. The SEM used was a JEOL JSM 5900LV fitted with a tungsten filament at an acceleration voltage of 15 kV and a working distance of about 10 mm. Samples were gold coated *in vacuo* with a Polaron SC7640 sputter coater fitted with a rotary planetary stage using a voltage of 2.2 kV and amperage of 25 mA for 3 min.

We categorized shell dissolution into 3 types based on the depth within the crystalline layer to which dissolution extended, following the methods described in Bednaršek et al. (2012c). Samples were chosen randomly and scored 'blindly' with no *a priori* knowledge of sample origin. Type I dissolution was characterized by slight dissolution within the upper prismatic layer and high shell porosity. Where aragonite crystals were exposed, the tips of the crystals appear to have 'cauliflower' heads occasionally present. Type II dissolution reflected erosion of the prismatic layer and damage protruding deeper into the underlying shell layers. The erosion of the upper-prismatic layer represented 20% of the shell mass crystalline structure. Type III dissolution affected the underlying crossed-lamellar layer, where the crystals have been partially dissolved and have become thicker and shorter. The extent of dissolution and porosity increased throughout the shell with higher levels of dissolution, resulting in a more fragile shell with less tightly organized crystals. Type II and Type III dissolution impacts shell fragility and we therefore refer to this kind of damage as severe (Bednaršek et al. 2012c); this type of dissolution is what we report on here. All organisms that demonstrated Type III dissolution also demonstrated some Type II dissolution, but the percentage of Type II dissolution was excluded from the Type III percentage. Prior to SEM, we positioned pteropod

shells with the whorls facing upward to scan the upper-shell surface. Using the same position and angle, we assured that the same upper-surface dissolution areas were always measured. This approach allowed for standardization between measurements across all individuals. Dissolution was quantified using image segmentation software (EDISON) that estimated the areal extent of each dissolution type in each image. Images were combined to determine overall coverage for each specimen. A detailed description and user guidelines on the procedure are given in Bednaršek et al. (2012c) in the supplementary information.

RESULTS

Frontal structure

The E-Front was apparent as a gradient in sea surface height (SSH) at the northeastern edge of an anticyclonic eddy in the southern California Current System (Fig. 1a). The feature was resolved repeatedly in subsurface profiling by SeaSoar, which crossed the frontal boundary at least 8 times. Fig. 1b illustrates changes in Ω_{arag} across the frontal region, where Ω_{arag} = 1 shoals from a depth of >200 m to the west of the E-Front to 50–75 m to the east of the front.

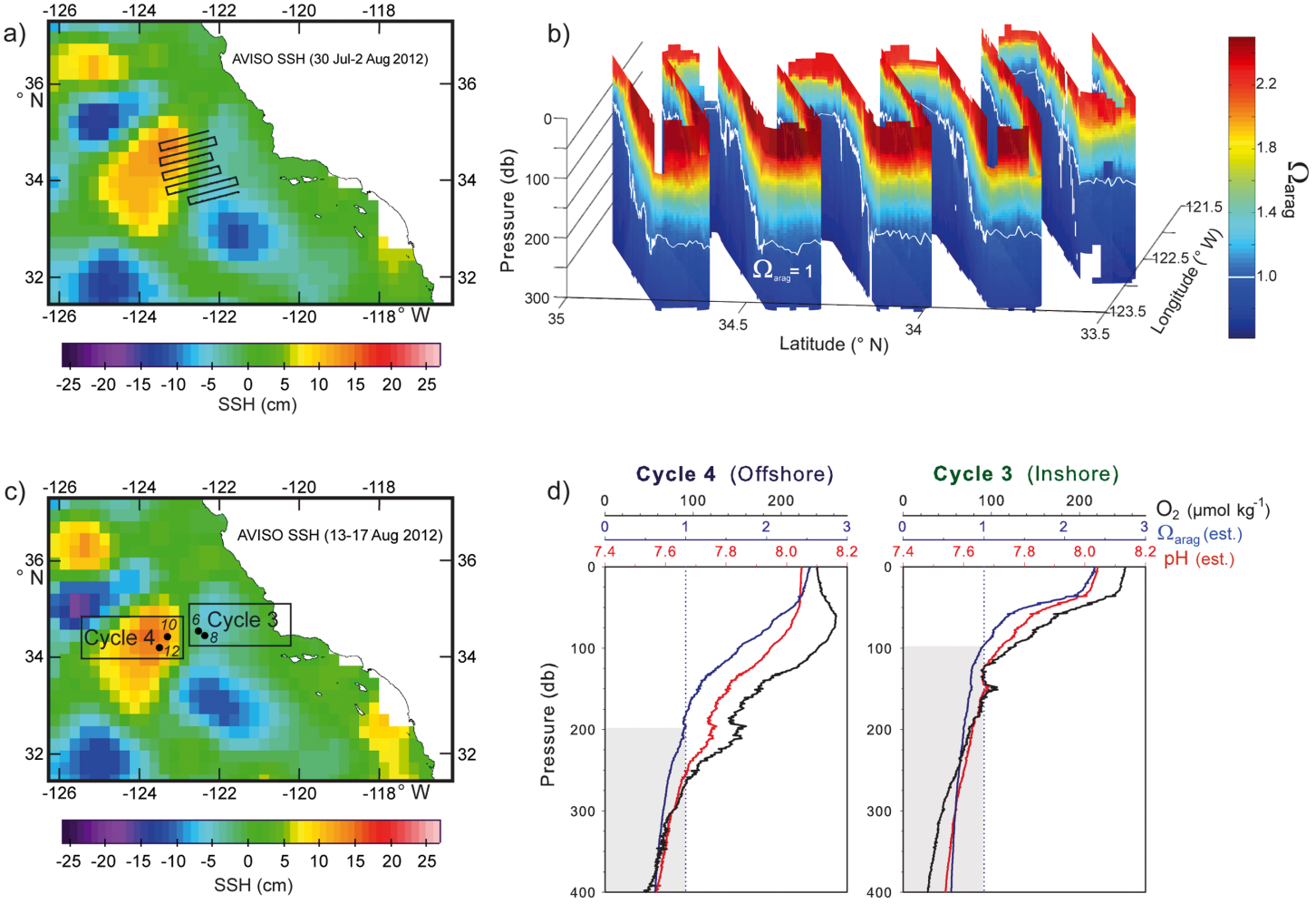

Fig. 1. Eddy front (E-Front) study site in the California Current System. (a) SeaSoar survey track (black lines) superimposed on an image of AVISO satellite sea surface height anomalies. (b) Sections of aragonite saturation state (Ω_{arag}) as a function of depth along the SeaSoar survey track. Ω_{arag} is derived from the relationship in Alin et al. (2012); white line indicates Ω_{arag} = 1.0. Note the rotation of the survey grid to illustrate repeated crossings of the E-Front. (c) Locations of MOCNESS samples at Cycle 3 (tows 6 and 8) and Cycle 4 (tows 10 and 12), located on either side of the E-Front. (d) Vertical profiles of dissolved oxygen, and estimated pH and Ω_{arag} (from Alin et al. 2012) at Cycle 4 (offshore of the E-Front) and Cycle 3 (inshore of the E-Front); 1 db of pressure ~ 1 m of depth. Shading indicates depths where Ω_{arag} < 1.0

Cross-frontal changes in temperature and oxygen (from which Ω_{arag} is derived) can be seen in Fig. S1 in the Supplement at www.int-res.com/articles/suppl/m523p093_supp.pdf.

Vertical profiles of hydrographic properties, dissolved oxygen, and inferred pH and Ω_{arag} were determined at the specific locations of pteropod sampling from sensors on the MOCNESS frame. At Cycle 4 (located to the west of the E-Front; Fig. 1c), Ω_{arag} was consistently <1.0 below a depth of 200 m. At Cycle 3 (to the east of the E-Front), undersaturated waters ($\Omega_{arag} < 1$) occurred at much shallower depths (~100 m; Fig. 1d). Vertical profiles of other variables at the MOCNESS sampling locations may be seen in Fig. S2 in the Supplement. Note that the anticyclonic eddy and associated E-Front moved slightly to the west in the 2 wk between the SeaSoar survey shown in Fig. 1a and the MOCNESS sampling in Fig. 1c, but the frontal feature remained sharp and clearly identifiable.

Pteropod and heteropod assemblages

The same species were present both inshore and offshore of the front: the thecosomes *Limacina helicina, Clio pyramidata* (Linnaeus, 1767), *Limacina bulimoides* (d'Orbigny, 1834), and *Limacina trochiformis* (d'Orbigny, 1834), the pseudothecosome *Peracle bispinosa* (Pelseneer, 1888) and the heteropod *Atlanta californiensis* (Seapy & Richter, 1993). *Heliconoides inflatus* (d'Orbigny, 1834, formerly *Limacina inflata*) and *Cavolinia uncinata* (d'Orbigny, 1834) were occasionally found, but rare. The dominant species was *L. helicina*, comprising 79% of total pteropod abundance, followed by *Clio pyramidata* (7%), while other species constituted no more than 4% of the total pteropod abundance. The integrated abundance of total pteropods and heteropods was about 50% greater in the offshore region, despite lower chlorophyll *a* (chl *a*) and light attenuation (Fig. S2 in the Supplement) and presumed lower food supply in the offshore region.

Vertical distributions of pteropods and heteropods differed on either side of the front. *L. helicina* was most concentrated in the upper 75 m of the water column in both regions (Fig. 2a,b). However, a somewhat larger fraction of the vertically integrated *L. helicina* population extended below 100 m depth (mean = 27%, range 17 to 36%) at Cycle 4, where the Ω_{arag} was deeper, than at Cycle 3 (mean = 17%, range 15 to 19%). The average body size of *L. helicina* (as shell length) increased 2.5 to 3 times from surface to deeper waters at both locations (Fig. 2c,d). At both locations, animals larger than 1.1 mm (on average) began to occur just below the depth of undersaturation, i.e. below 200 m offshore at Cycle 4 and below 100 to 150 m inshore at Cycle 3.

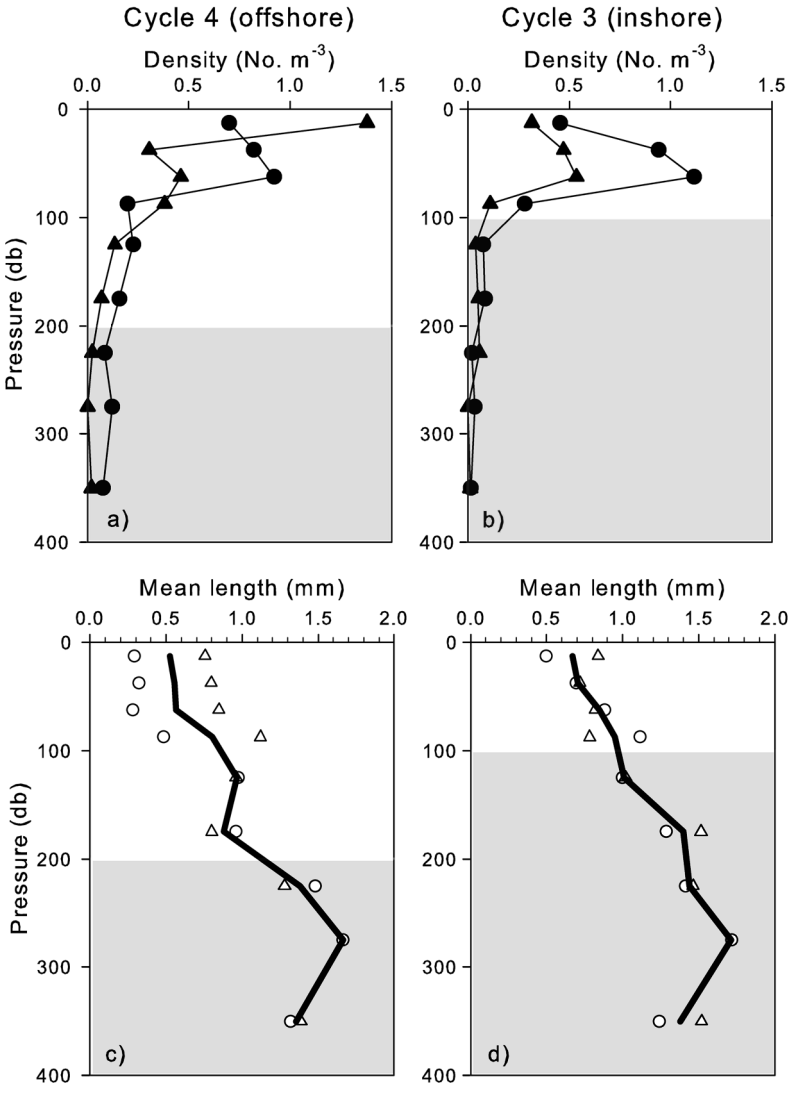

Fig. 2. Vertical distributions of the thecosome pteropod *Limacina helicina* at Cycle 4 and Cycle 3 indicating (a,b) population density and (c,d) mean shell length. Circles: tows 10 and 6; triangles: tows 12 and 8. Shading indicates depths where $\Omega_{arag} < 1.0$

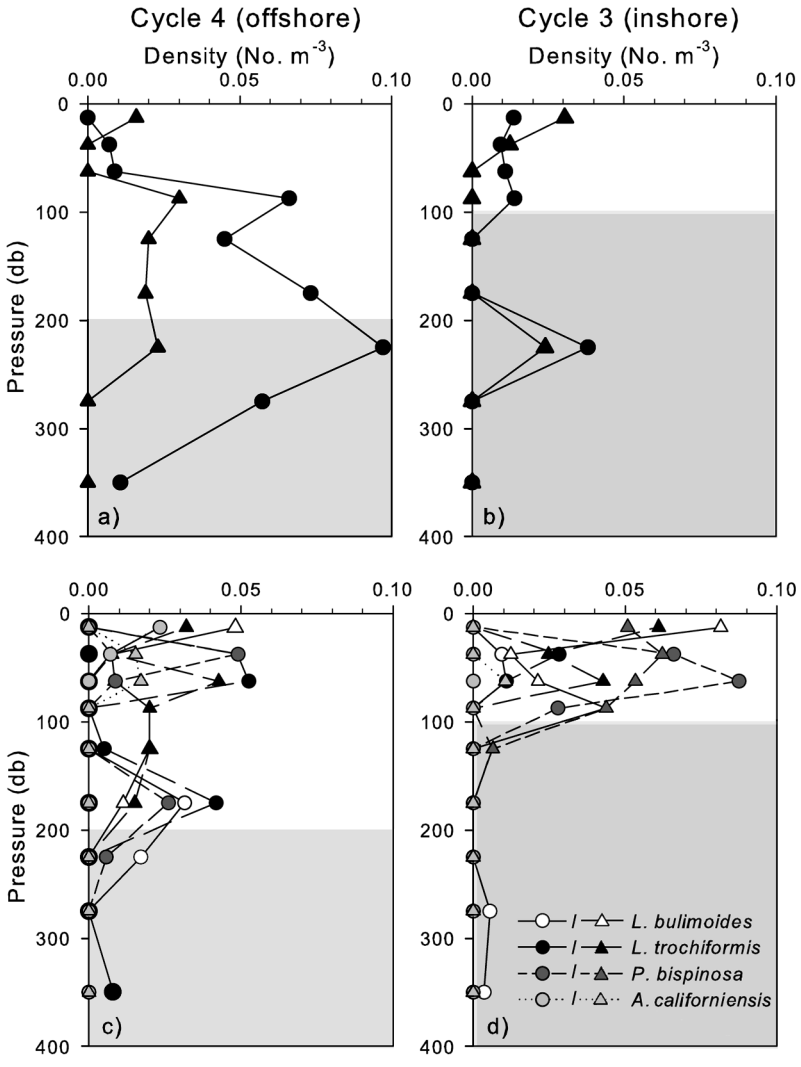

Fig. 3. Vertical distributions of (a,b) the thecosome pteropod *Clio pyramidata* and (c,d) other taxa (the thecosomes *Limacina bulimoides, Limacina trochiformis*, and *Peracle bispinosa*, and the heteropod *Atlanta californiensis*) at Cycle 4 and Cycle 3. Circles: tows 10 and 6; triangles: tows 12 and 8. Shading indicates depths where $\Omega_{arag} < 1.0$

Waters deeper than 250 m contained a relatively small number of *L. helicina*, but these individuals were the largest in average size.

C. pyramidata was more broadly distributed throughout the water column, with elevated subsurface abundances on both sides of the front (Fig. 3a,b). However, a higher proportion of animals in waters deeper than 100 m occurred on the offshore side (mean = 80%, range 73 to 88%) than the onshore side (mean = 57%, range 53 to 61%). Other pteropod taxa were considerably less abundant, but showed a consistent pattern of deeper vertical extent into 100 or 200 m depths on the offshore side of the front (Fig. 3c,d). The heteropod *A. californiensis* was quite sparse and occurred only in the upper 75 m at both cycles. The proportion of pteropods found between 100 and 200 m depth was a significantly greater fraction of the total vertically integrated population at Cycle 4 than at Cycle 3 ($p < 0.05$; Wilcoxon matched pairs test). Similarly, the proportion of pteropods found below 100 m depth was a greater fraction of the vertically integrated population ($p < 0.05$) at Cycle 4.

Sufficient specimens of *L. helicina* were available to assess shell dissolution as a function of depth. Intact, undamaged shell surfaces are illustrated in Fig. 4a, with the slight pitting typical of Type I dissolution seen in Fig. 4e. More severe dissolution is reflected by Type II (Fig. 4b) and Type III (Fig. 4c,d) dissolution. Some Type I level dissolution was seen in *L. helicina* from all depths, ranging from 20 to 90% of the shell surface (data not shown). Type II and III dissolution of *L. helicina* shells varied strongly as a function of depth (Fig. 5a,b; $p < 0.0001$, Jonckheere's test for ordered alternatives). Peak dissolution occurred near the saturation depth horizon where $\Omega_{arag} = 1$, i.e. near 200 m at Cycle 4 and 100 m at Cycle 3 (Fig. 5a,b). The maximum area of dissolved shell surface was 29 and 50% (Type II dissolution) at Cycles 4 and 3, respectively, and 38 and 20% (Type III dissolution) at Cycles 4 and 3, respectively. In deeper waters where $\Omega_{arag} < 1$, the percentage of shell dissolution did not differ between Cycles 4 and 3 ($p > 0.10$, both Types II and III dissolution; Mann-Whitney *U*). Shell dissolution diminished in shallower waters in both regions (Fig. 5a,b). At depths where $\Omega_{arag} > 1$, shell dissolution was greater inshore of the front at Cycle 3 for both Type II ($p < 0.00001$) and Type III dissolution ($p < 0.05$; Mann-Whitney *U*). Percent shell dissolution did not vary significantly with depth in deeper waters where $\Omega_{arag} < 1.0$ (Kruskal-Wallis; $p > 0.10$), i.e. >200 m at Cycle 4 and >100 m at Cycle 3. Plotted as a function of average Ω_{arag} in each of the sampled depth strata (Fig. 5c,d), both Type II and Type III dissolution were close to maximal in the stratum where Ω_{arag} first reached 1.0, declining gradually at higher saturation states.

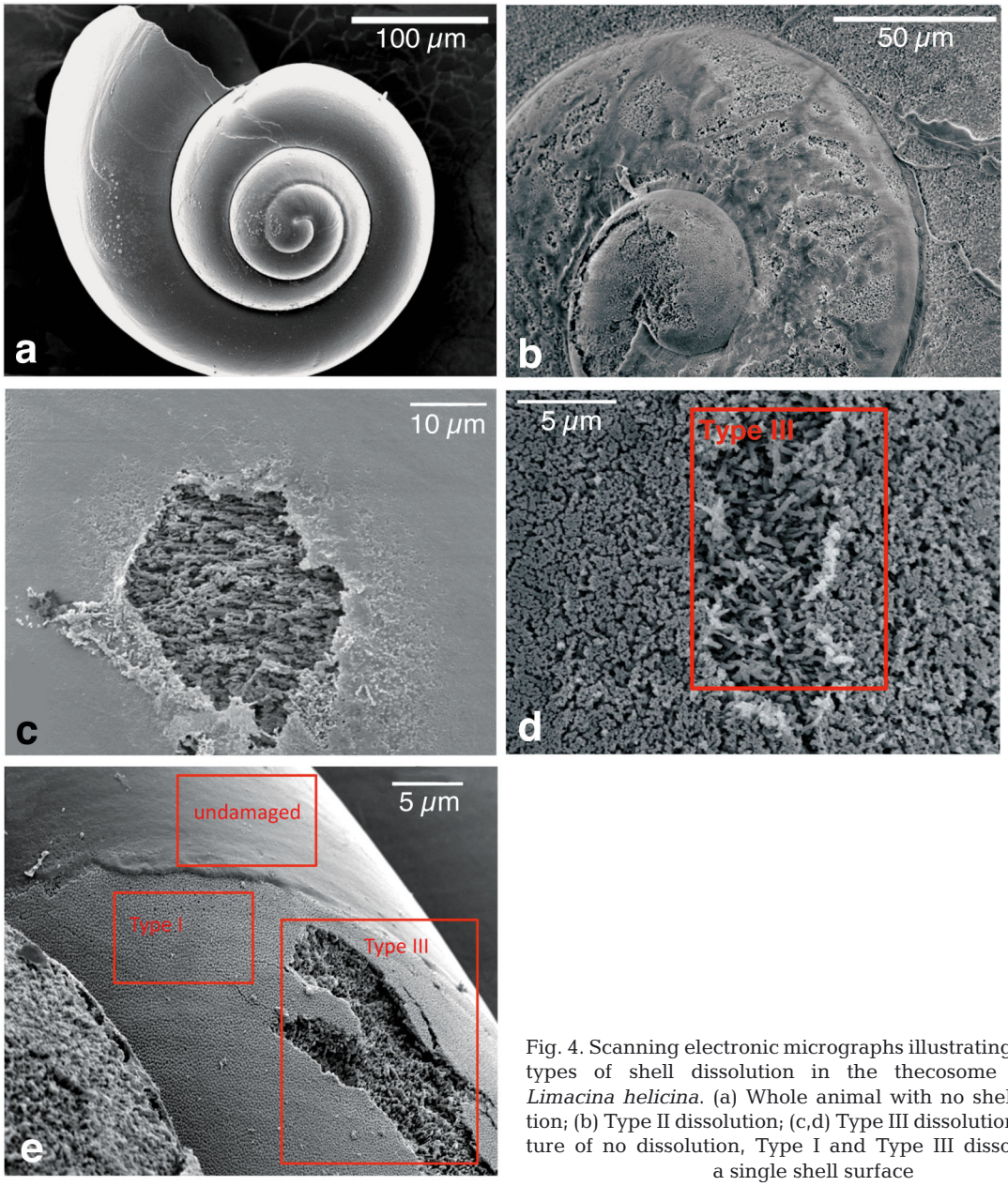

Fig. 4. Scanning electronic micrographs illustrating different types of shell dissolution in the thecosome pteropod *Limacina helicina*. (a) Whole animal with no shell dissolution; (b) Type II dissolution; (c,d) Type III dissolution; (e) mixture of no dissolution, Type I and Type III dissolution on a single shell surface

DISCUSSION

Pteropods in the southern California Current System inhabit a coastal upwelling biome that is forced by physical processes on different time and space scales, resulting in a changing environment with respect to carbonate chemistry. One source of spatial structuring in this ecosystem is the presence of ocean fronts, where relatively abrupt changes may be seen in hydrographic and biotic variables over small spatial scales (Davis et al. 2008, Ohman et al. 2012, Powell & Ohman 2015). Here, we illustrate that aragonite saturation horizons (Ω_{arag} = 1) can change from a depth of more than 200 m to less than 75 m across a persistent eddy-related front, as temperature and dissolved oxygen change abruptly across this gradient. These changes alter the geochemical environment for shell-bearing pteropods, heteropods, and other calcifying organisms. Comparable or greater vertical changes in aragonite saturation conditions are well known from the California Current System (Feely et al. 2008, Alin et al. 2012, Ohman et al.

2013b), but on much larger spatial scales than analyzed here.

These geochemical changes were associated with cross-frontal differences in vertical distributions of several species of pteropods, as reflected in more limited occupation of the depth stratum between 100 and 200 m in a location where waters were undersaturated with respect to aragonite (i.e. Ω_{arag} < 1). Shoaling of the undersaturated waters was associated with a compression of the vertical habitat occupied by a majority of the population. Species varied in the extent of habitat compression, depending on the proportion of the population that would otherwise occupy deeper depths where saturated waters occur. Only the heteropod *Atlanta californiensis* was not directly affected, because it was found exclusively in shallow depth strata, although we note it was too rare in these samples to accurately assess subsurface distributions.

While we cannot establish unequivocally that the changes in habitat were attributable to changes in geochemical variables alone, several lines of evidence suggest that carbonate chemistry is a dominant controlling factor. First, integrated total abundances are somewhat higher in the offshore region of supersaturated conditions, suggesting that the offshore region may be a more favorable habitat. Although our total number of profiles was limited here, this same pattern of elevated abundances of pteropods farther from shore in upwelling areas also occurs repeatedly along established CalCOFI sampling lines (M. D. Ohman unpubl. data). Farther north in the California Current System, Mackas & Galbraith (2012) also reported that *Limacina* spp. are, on average, more abundant in offshore waters than in proximity to Vancouver Island. Concerning the possible role of temperature in affecting pteropod distributions in our study site, temperatures were 1 or

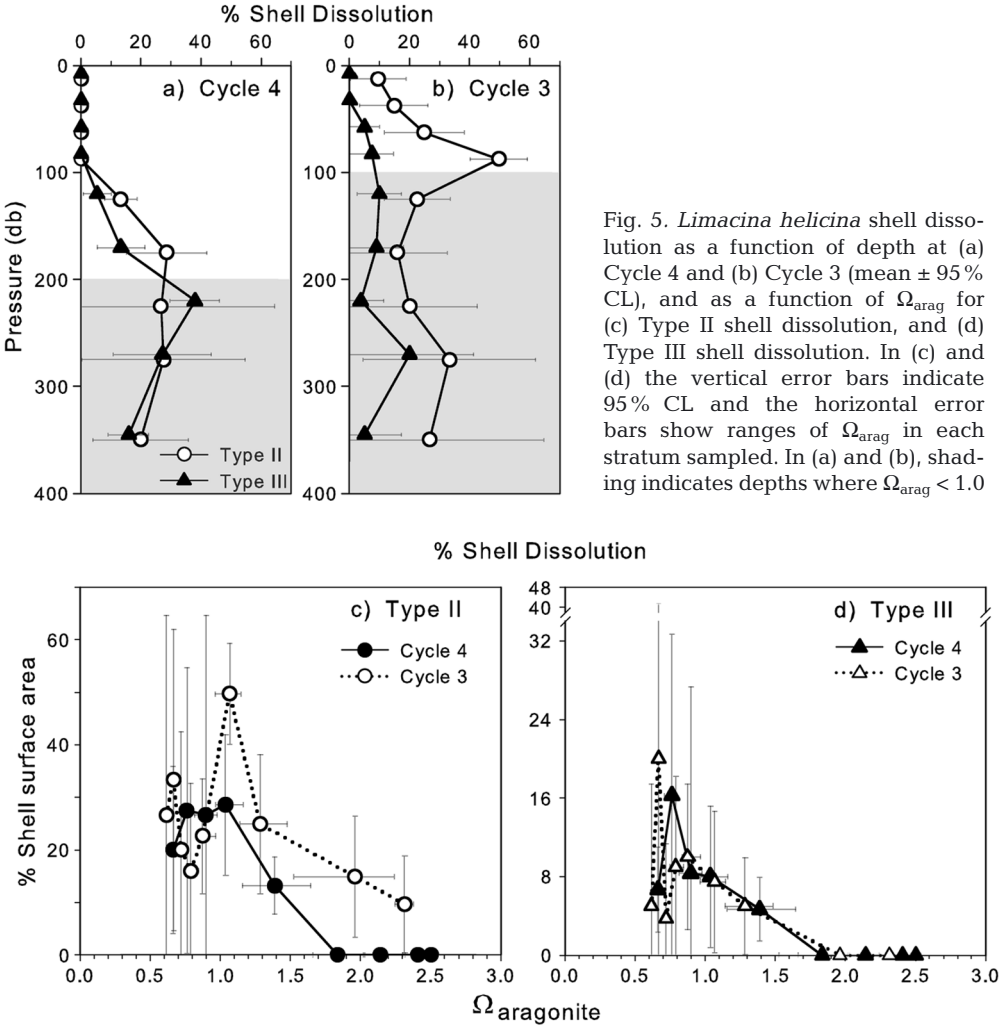

Fig. 5. *Limacina helicina* shell dissolution as a function of depth at (a) Cycle 4 and (b) Cycle 3 (mean ± 95% CL), and as a function of Ω_{arag} for (c) Type II shell dissolution, and (d) Type III shell dissolution. In (c) and (d) the vertical error bars indicate 95% CL and the horizontal error bars show ranges of Ω_{arag} in each stratum sampled. In (a) and (b), shading indicates depths where Ω_{arag} < 1.0

2°C lower inshore of the E-Front. However, such temperatures are well within the tolerances of these pteropods and are unlikely to be inhibitory or impose changes in pteropod behavior for temperate pteropods over a short time window (Dadon & de Cidre 1992, Bednaršek et al. 2012b). Our measured dissolved oxygen concentrations exceeded hypoxic levels throughout the water column in both sampled regions. However, while we cannot exclude dissolved oxygen as an additional factor limiting vertical distributions at either location, dissolved oxygen cannot explain the shell dissolution we observed. Particulate food supply for pteropods, as inferred indirectly from chl *a* fluorescence and from the beam attenuation coefficient (which is proportional to light scattering by total particulates in the water column, and related to particulate organic carbon; Bishop 1999), was higher in the inshore region, suggesting pteropods were not limited by food availability on the inshore side of the front. Although it is difficult to quantify predation risk, visual predators would be expected to hunt more effectively in the optically clearer offshore waters, yet thecosomes are slightly more abundant there. Furthermore, in addition to patterns of abundance, the covariability of vertical distribution of *Limacina helicina* shell dissolution with Ω_{arag} suggests that the geochemical environment directly influences pteropod shell dissolution, similar to what we have observed elsewhere (Bednaršek et al. 2012a, 2014). Hence, we infer that variations in aragonite saturation across the front studied here did influence the vertical distributions and shell characteristics of thecosome pteropods.

Our results indicate that severe shell dissolution of *L. helicina* is most pronounced at depths corresponding to $\Omega_{arag} < 1.2$ to 1.4, with appreciably less evidence of shell dissolution in shallower, more saturated waters. Bednaršek et al. (2012a,c) demonstrated that dissolution is not restricted to $\Omega_{arag} < 1$, but can start occurring at $\Omega_{arag} \sim 1.1$ to 1.2. It is noteworthy that even at depths where Ω_{arag} was > 2.0 in the present study, some shell dissolution was detectable, especially at Cycle 3 inshore of the front. These results suggest that a threshold value of Ω_{arag} for shell dissolution can be considerably greater than 1.0.

Pteropods collected at Cycle 4 were sampled from the interior of a relatively stable anticyclonic eddy that existed for at least 2 mo prior to our sampling, and persisted for at least an additional 2 to 3 mo afterward (M. Kahru pers. comm., from analysis of AVISO satellite imagery). Hence, it is likely that the aragonite saturation conditions in the waters at the time of sampling were reflective of what animals had experienced for at least the preceding 2 mo. Pteropods analyzed from Cycle 3 were not sampled in a retentive physical feature. Cycle 3 was part of the open coastal circulation, so that animals sampled at that location could previously have experienced less saturated waters closer to the coast. Therefore, it is possible that the saturation states that we measured at the time of pteropod sampling may not fully reflect the geochemical environment experienced throughout the earlier development of these animals, especially at Cycle 3.

The vertical distributions analyzed here reflect only daytime occurrence of the pteropods, while some of these species are known to undergo diel vertical migrations (e.g. Mackas & Galbraith 2002, Nigro & Seapy 2008) in the North Pacific, and related species elsewhere (e.g. Wormuth 1981, Lalli & Gilmer 1989, Hunt et al. 2008). Daytime distributions were the appropriate focus for the present analysis because they reflect the deepest depths occupied during a 24 h period and are therefore most relevant to testing relationships with Ω_{arag}. The least saturated (hence most potentially corrosive) waters will be experienced in deeper strata, by day. However, there is some limited evidence for size-dependent diel vertical migration of some thecosomes, where the largest bodied individuals tend to exhibit the largest amplitude migrations (cf. Nigro & Seapy 2008). If diel vertical migration in species such as *L. helicina* varies with body size, leading larger-bodied pteropods to undergo larger amplitude vertical migrations than smaller animals, the large-bodied, deeper-dwelling animals may experience less corrosive conditions than expected from daytime conditions alone. If the largest-bodied animals spend only part of the day in deep, undersaturated waters and part in supersaturated waters near the surface, the geochemical degradation of shells may be diminished in comparison with degradation that would occur if these individuals resided continuously in undersaturated waters throughout a 24 h period. In addition, in larger-sized individuals, shell structure gains structural and mechanical properties during development that may retard chemical dissolution and resist mechanical degradation (Harper 2000, Sato-Okoshi et al. 2010). It is also possible that adults have an efficient repair system of calcification (e.g. Lischka et al. 2011) which could offset some early stages of dissolution.

The severe dissolution detected here was consistent with the extent of dissolution described by Bednaršek et al. (2012a) for near-saturated ($\Omega_{ar} \sim 1$) exposure for 8 d. However, those and other published

experiments treating shell dissolution have been conducted with continuous exposure to undersaturated conditions (Orr et al. 2005, Comeau et al. 2010, Lischka et al. 2011). It is not yet known whether regular alternating exposure to undersaturated and supersaturated conditions over a 24 h period either mitigates shell dissolution or extends the cumulative exposure time to undersaturated conditions that would be required to degrade shell structure. Our hypothesis of reduced shell dissolution during periodic exposure to supersaturated conditions over a 24 h cycle is amenable to direct experimental testing.

Our analysis of abrupt, front-related changes in Ω_{arag} exploited natural gradients of carbonate chemistry that are as yet unachievable under experimental or mesocosm conditions because of the large vertical extent (>300 m) of some pteropod distributions. Our results suggest restrictions in volume of mesopelagic habitat occupied by several thecosome pteropods, associated with the shoaling of undersaturated waters. This habitat compression into shallower saturated waters would alter both the food and predation environment experienced by these organisms in near-surface waters with increasing ocean acidification. Occupation of progressively shallower waters could expose animals to increasing predation risk by sight-hunting feeding predators, as has been suggested for organisms affected by shoaling hypoxic boundaries (e.g. Koslow et al. 2011). In the California Current System, however, there is also a long-term trend toward reduced transparency of surface waters (Aksnes & Ohman 2009), which could partially mitigate the increased predation exposure accompanying habitat compression. Such population level effects on the vertical distributions of thecosome pteropods and heteropods need to be considered in future projections of changes in water column geochemistry.

Acknowledgements. We express appreciation to the National Research Council, the NOAA Pacific Marine Environmental Laboratory and the NOAA Ocean Acidification Program for financial support of N.B. Shiptime was supported by NSF. We thank R.A. Feely for discussions, insights, and assistance throughout these analyses, and for comments on the manuscript. We thank all participants in CCE-LTER P1208 for their cooperation and assistance at sea. David Jensen provided expert programming, Linsey Sala provided assistance in the SIO Pelagic Invertebrates Collection, Mati Kahru processed satellite imagery, and Carl Mattson and Alain de Verneil led the SeaSoar Survey. Thanks are also extended to Michael Landry for his role as Chief Scientist. A contribution from the California Current Ecosystem Long Term Ecological Research site, supported by the US NSF. PMEL contribution no. 4166.

LITERATURE CITED

Accornero A, Manno C, Esposito F, Gambi MC (2003) The vertical flux of particulate matter in the polynya of Terra Nova Bay. Part II. Biological components. Antarct Sci 15: 175–188

Aksnes DL, Ohman MD (2009) Multi-decadal shoaling of the euphotic zone in the southern sector of the California Current System. Limnol Oceanogr 54:1272–1281

Alin SR, Feely RA, Dickson A, Hernandez-Ayon JM, Juranek LW, Ohman MD, Goericke R (2012) Robust empirical relationships for estimating the carbonate system in the southern California Current System and application to CalCOFI hydrographic cruise data (2005-2011). J Geophys Res 117:C05033, doi:10.1029/2011JC007511

Barton A, Hales B, Waldbusser GG, Langdon C, Feely RA (2012) The Pacific oyster, *Crassostrea gigas*, shows negative correlation to naturally elevated carbon dioxide levels: implications for near-term ocean acidification effects. Limnol Oceanogr 57:698–710

Bednaršek N, Tarling GA, Bakker DCE, Fielding S and others (2012a) Extensive dissolution of live pteropods in the Southern Ocean. Nat Geosci 5:881–885

Bednaršek N, Možina J, Vogt M, O'Brien C, Tarling GA (2012b) The global distribution of pteropods and their contribution to carbonate and carbon biomass in the modern ocean. Earth Syst Sci Data 4:167–186

Bednaršek N, Tarling GA, Bakker DC, Fielding S and others (2012c) Description and quantification of pteropod shell dissolution: a sensitive bioindicator of ocean acidification. Glob Change Biol 18:2378–2388

Bednaršek N, Feely RA, Peterson W, Reum J, Alin SR, Hales B (2014) Impact of ocean acidification on *Limacina helicina* shell dissolution in the California Current System. Proc R Soc B

Bishop JKB (1999) Transmissometer measurement of POC. Deep-Sea Res II 46:353–369

Bograd SJ, Buil MP, Di Lorenzo E, Castro CG and others (2014) Changes in source waters to the Southern California Bight. Deep-Sea Res II 112:42–52

Chan F, Barth JA, Lubchenco J, Kirincich A, Weeks H, Peterson WT, Menge BA (2008) Emergence of anoxia in the California Current Large Marine Ecosystem. Science 319:920

Comeau S, Gorsky G, Jeffree R, Teyssie JL, Gattuso JP (2009) Impact of ocean acidification on a key Arctic pelagic mollusc (*Limacina helicina*). Biogeosciences 6: 1877–1882

Comeau S, Gorsky G, Alliouane S, Gattuso JP (2010) Larvae of the pteropod *Cavolinia inflexa* exposed to aragonite undersaturation are viable but shell-less. Mar Biol 157: 2341–2345

Dadon JR, de Cidre LL (1992) The reproductive cycle of the thecosomatous pteropod *Limacina retroversa* in the western South Atlantic. Mar Biol 114:439–442

Davis RE, Ohman MD, Rudnick DL, Sherman JT, Hodges B (2008) Glider surveillance of physics and biology in the southern California Current System. Limnol Oceanogr 53:2151–2168

Di Lorenzo E, Ohman MD (2013) A double-integration hypothesis to explain ocean ecosystem response to climate forcing. Proc Natl Acad Sci USA 110:2496–2499

Doney SC, Balch WM, Fabry VJ, Feely RA (2009) Ocean acidification: a critical emerging problem for the ocean sciences. Oceanography 22:16–25

Fabry VJ, Seibel BA, Feely RA, Orr JC (2008) Impacts of ocean acidification on marine fauna and ecosystem processes. ICES J Mar Sci 65:414–432

Fassbender AJ, Sabine CL, Feely RA, Langdon C, Mordy CW (2011) Inorganic carbon dynamics during northern California coastal upwelling. Cont Shelf Res 31: 1180–1192

Feely RA, Sabine CL, Lee K, Berelson W, Kleypas J, Fabry VJ, Millero FJ (2004) Impact of anthropogenic CO_2 on the $CaCO_3$ system in the oceans. Science 305:362–366

Feely RA, Sabine CL, Hernandez-Ayon JM, Ianson D, Hales B (2008) Evidence for upwelling of corrosive 'acidified' water onto the continental shelf. Science 320:1490–1492

Gruber N, Hauri C, Lachkar Z, Loher D, Froelicher TL, Plattner GK (2012) Rapid progression of ocean acidification in the California Current System. Science 337:220–223

Harper EM (2000) Are calcitic layers an effective adaptation against shell dissolution in the Bivalvia? J Zool 251: 179–186

Harris KE, DeGrandpre MD, Hales B (2013) Aragonite saturation state dynamics in a coastal upwelling zone. Geophys Res Lett 40:2720–2725

Hauri C, Gruber N, Plattner GK, Alin S, Feely RA, Hales B, Wheeler PA (2009) Ocean acidification in the California Current System. Oceanography 22:60–71

Hauri C, Gruber N, McDonnell AMP, Vogt M (2013) The intensity, duration, and severity of low aragonite saturation state events on the California continental shelf. Geophys Res Lett 40:3424–3428

Hunt BPV, Pakhomov EA, Hosie GW, Siegel V, Ward P, Bernard K (2008) Pteropods in Southern Ocean ecosystems. Prog Oceanogr 78:193–221

Johnston TMS, Rudnick DL, Pallàs-Sanz E (2011) Elevated mixing at a front. J Geophys Res 116:C11033, doi: 10.1029/2011JC007192

Koslow JA, Goericke R, Lara-Lopez A, Watson W (2011) Impact of declining intermediate-water oxygen on deep-water fishes in the California Current. Mar Ecol Prog Ser 436:207–218

Lachkar Z (2014) Effects of upwelling increase on ocean acidification in the California and Canary Current systems. Geophys Res Lett 41:90–95

Lalli CM, Gilmer RW (1989) Pelagic snails: the biology of holoplanktonic gastropod mollusks. Stanford University Press, CA

Lavaniegos BE, Ohman MD (2007) Coherence of long-term variations of zooplankton in two sectors of the California Current System. Prog Oceanogr 75:42–69

Lischka S, Budenbender J, Boxhammer T, Riebesell U (2011) Impact of ocean acidification and elevated temperatures on early juveniles of the polar shelled pteropod *Limacina helicina*: mortality, shell degradation, and shell growth. Biogeosciences 8:919–932

Mackas DL, Galbraith MD (2002) Zooplankton distribution and dynamics in a North Pacific eddy of coastal origin: 1. Transport and loss of continental margin species. J Oceanogr 58:725–738

Mackas DL, Galbraith MD (2012) Pteropod time-series from the NE Pacific. ICES J Mar Sci 69:448–459

Manno C, Tirelli V, Accornero A, Umani SF (2010) Importance of the contribution of *Limacina helicina* faecal pellets to the carbon pump in Terra Nova Bay (Antarctica). J Plankton Res 32:145–152

Martz T, Send U, Ohman MD, Takeshita Y, Bresnahan P, Kim HJ, Nam S (2014) Dynamic variability of biogeochemical ratios in the southern California Current System. Geophys Res Lett 41:2496–2501

Niehoff B, Schmithuesen T, Knueppel N, Daase M, Czerny J, Boxhammer T (2013) Mesozooplankton community development at elevated CO_2 concentrations: results from a mesocosm experiment in an Arctic fjord. Biogeosciences 10:1391–1406

Nigro DT, Seapy RR (2008) Diel patterns of vertical distribution in euthecosomatous pteropods of Hawaiian waters. Veliger 50:190–209

Ohman MD, Lavaniegos BE, Townsend AW (2009) Multidecadal variations in calcareous holozooplankton in the California Current System: thecosome pteropods, heteropods, and foraminifera. Geophys Res Lett 36: L18608, doi:10.1029/2009gl039901

Ohman MD, Powell JR, Picheral M, Jensen DW (2012) Mesozooplankton and particulate matter responses to a deep-water frontal system in the southern California Current System. J Plankton Res 34:815–827

Ohman MD, Barbeau K, Franks PJS, Goericke R, Landry MR, Miller AJ (2013a) Ecological transitions in a coastal upwelling ecosystem. Oceanography 26:210–219

Ohman MD, Rudnick DL, Chekalyuk A, Davis RE and others (2013b) Autonomous ocean measurements in the California Current Ecosystem. Oceanography 26:18–25

Orr JC, Fabry VJ, Aumont O, Bopp L and others (2005) Anthropogenic ocean acidification over the twenty-first century and its impact on calcifying organisms. Nature 437:681–686

Powell JR, Ohman MD (2015) Co-variability of zooplankton gradients with glider-detected density fronts in the southern California Current System. Deep-Sea Res II 112:79–90

Roberts D, Howard WR, Moy AD, Roberts JL, Trull TW, Bray SG, Hopcroft RR (2011) Interannual pteropod variability in sediment traps deployed above and below the aragonite saturation horizon in the sub-Antarctic Southern Ocean. Polar Biol 34:1739–1750

Rykaczewski RR, Dunne JP (2010) Enhanced nutrient supply to the California Current Ecosystem with global warming and increased stratification in an earth system model. Geophys Res Lett 37:L21606, doi:10.1029/2010GL045019

Sato-Okoshi W, Okoshi K, Sasaki H, Akiha F (2010) Shell structure of two polar pelagic molluscs, Arctic *Limacina helicina* and Antarctic *Limacina helicina antarctica* forma *antarctica*. Polar Biol 33:1577–1583

Schulz KG (2013) Coccolithophorid blooms at elevated levels of carbon dioxide: new insights from mesocosm studies. Phycologia 52S:99 (Abstract)

Teniswood CMH, Roberts D, Howard WR, Bradby JE (2013) A quantitative assessment of the mechanical strength of the polar pteropod *Limacina helicina antarctica* shell. ICES J Mar Sci 70:1499–1505

Waldbusser GG, Brunner EL, Haley BA, Hales B, Langdon CJ, Prahl FG (2013) A developmental and energetic basis linking larval oyster shell formation to acidification sensitivity. Geophys Res Lett 40:2171–2176

Wiebe PH, Morton AW, Bradley AM, Backus RH and others (1985) New developments in the MOCNESS, an apparatus for sampling zooplankton and micronekton. Mar Biol 87:313–323

Wormuth JH (1981) Vertical distributions and diel migrations of Euthecosomata in the northwest Sargasso Sea. Deep-Sea Res Part A 28:1493–1515

Editorial responsibility: Marsh Youngbluth, Fort Pierce, Florida, USA

Submitted: July 28, 2014; Accepted: January 12, 2015
Proofs received from author(s): March 3, 2015